ELSEVIER

Biophysical Chemistry 67 (1997) 59–64

Biophysical Chemistry

Evidence for increased proton dissociation in low-activity forms of dephosphorylated squash-leaf nitrate reductase

Peter Ruoff *, Cathrine Lillo

Stavanger College, School of Technology and Science, P.O. Box 2557 Ullandhaug, 4004 Stavanger, Rogaland, Norway

Received 22 January 1997; revised 11 April 1997; accepted 11 April 1997

Abstract

The pH dependence of squash-leaf nitrate reductase has been studied. It has been found that high- and low-activity forms of purified nitrate reductase (both forms dephosphorylated) have different optimum pH values. A high-activity form has always a higher pH optimum compared with a low-activity form. Model computations show that the decrease in activity and the corresponding change of the pH optimum is apparently due to a conformation-dependent increase of proton dissociation of the enzyme. As previously shown, this behavior is also observed in leaf extracts during the conversion (and probably phosphorylation of nitrate reductase) from a high-active form to a low-active form when plants are transferred from light to darkness. © 1997 Elsevier Science B.V.

Keywords: Nitrate reductase; pH: Kinetics; *Cucurbita maxima* (squash)

1. Introduction

Nitrate reductase (NR) catalyzes the reduction of nitrate to nitrite.

$$NADH + H^+ + NO_3^- \xrightarrow{NR} NAD^+ + NO_2^- + H_2O \quad (R1)$$

This process is rate-determining in the assimilation of nitrate to organically bound nitrogen in higher plants and algae, and is therefore considered as one of the regulating steps in nitrogen metabolism. The activity of nitrate reductase is regulated at the transcriptional level [1,2], but fine tuning of activity at the posttranslational level is also of physiological importance [3–9].

NADH:nitrate reductase is a composite enzyme which consists of two identical monomer units. Each monomer contains FAD, heme and molybdenum pterin-binding domains (Fig. 1). One way of regulating nitrate reductase appears by phosphorylation at a conserved serine (located in the hinge between heme and molybdenum pterin-binding domains, Fig. 1) in the presence of Mg^{2+} and inhibiting proteins [10,11] when plants are exposed to darkness. Nitrate reductase-inhibiting proteins (NIP) have recently been identified to belong to the 14-3-3 family [12,13].

We have previously shown [14] that purified nitrate reductase has hysteretic properties [15–17], i.e., the enzyme interconverts slowly between high- and low-activity forms. It has now been found that the purified enzyme showing hysteresis is not phosphorylated at the regulatory serine site. In this paper, we show that nonphosphorylated high- and low-activity

* Corresponding author.

PII S0301-4622(97)00054-9

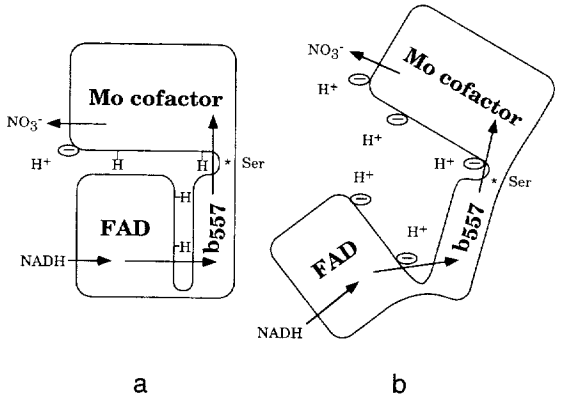

Fig. 1. Schematic representation of higher plant nitrate reductase monomer. Arrows indicate electron flow from NADH through FAD domain, b_{557} and Mo-cofactor to NO_3^- [1]. The asterisk indicates the hinge between b_{557} and Mo-cofactor binding domains where the regulatory serine is located. (a) 'Closed' conformation; (b) 'Open' conformation. An increase of $K_B^{E(S)}$ can be understood as a consequence of the open structure and an easier dissociation of the protons in the reacting solution. For discussion, see Sections 1 and 3.3.

forms of purified nitrate reductase have different optimum (assay) pH values. A high-activity form has always a higher pH optimum compared with a low-activity form. Model computations show that the decrease in activity and the corresponding change of the pH optimum is due to a conformation-dependent increase of proton dissociation of the enzyme. Interestingly, this behavior is not only observed for the dephosphorylated purified enzyme, but also in leaf extracts during the conversion (and probable phosphorylation) of a high-active nitrate reductase form to a low-active form when plants are transferred from light to darkness [18]. Based on these observations a schematic conformational model for the low- and high-activity forms of nitrate reductase is proposed.

2. Materials and methods

2.1. Cultivation of plants and enzyme preparation

Squash plants (*Cucurbita maxima*) were grown and harvested as described earlier [14]. Nitrate reductase was purified [14] with affinity chromatography using blue sepharose and hydroxylapatite from light-treated plants and stored initially at pH 7.5 in 25 mM tris–HCl buffer with 7 mM cysteine and 0.2 mM EDTA. Nitrate reductase was purified 800-fold with a specific activity of 12 units/mg protein [14]. One unit of nitrate reductase is defined as the rate of 1 μmol of nitrite produced in 1 min. Studies with NIP and Mg^{2+} showed that this form of nitrate reductase appears not to be phosphorylated (see below). Enzyme from this purification was also compared with a preparation where an additional immunological purification step [19] using a sepharose-immobilized antibody against NR was included. No differences in the hysteretic properties between the immunological and the blue sepharose preparations were detected indicating that the blue sepharose preparation gives an adequate description of the hysteretic properties of squash nitrate reductase.

Initial velocities v_0 of process R1 were determined by measuring spectrophotometrically at 540 nm the amount of nitrite ion produced as the diazo compound formed from sulfanilamide [20].

2.2. Diprotic model

This model is well-established [21–25] and used to describe bell-shaped activity–pH curves. The enzyme is considered as a diprotic acid EH_2, but only species EH^- and EHS^- are catalytically active. $K_A^{E(S)}$ and $K_B^{E(S)}$ are dissociation constants of the first and second dissociation steps of enzyme species EH_2 and EH_2S, respectively, while k_1, k_{-1} and k_2 are rate constants for the catalytically active reactions.

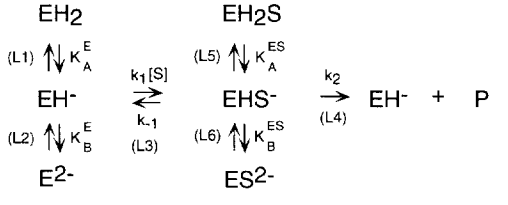

Rapid equilibrium assumption for steps L1, L2,

L5 and L6 together with a steady-state assumption for species EHS^- leads to the rate equation:

$$v = \frac{\left(\frac{V_{max}}{M_2}\right) \cdot [S]}{K_M\left(\frac{M_1}{M_2}\right) + [S]} \quad (1)$$

with $V_{max} = k_2[E]_t$, $M_1 = 1 + ([H^+])/(K_A^E) + (K_B^E)/([H^+])$, $M_2 = 1 + ([H^+])/(K_A^{ES}) + (K_B^{ES})/([H^+])$ and $K_M = (k_2 + k_{-1})/(k_1)$. $[E]_t$ is the total concentration of the enzyme.

3. Results and discussion

3.1. Activity-dependence on storage pH

In order to assure identical amounts of enzyme at different storage conditions, a batch of purified nitrate reductase was divided into two aliquots. In these aliquots the storage buffer was changed to either K–phosphate buffer (or to tris, hepes or bis,tris–propane buffers) of different pH values. Enzyme from both aliquots were taken and initial velocities were determined at different assay pH values in the range 6.5–8.5. Interestingly, at low assay pH, initial velocities v_0 approached the same activity–pH curve and reaction velocities were practically independent of the storage buffer's pH. At high-assay pH, initial velocities became markedly different and a 'splitting' of the v_0–pH curve occurred (Fig. 2a). This 'splitting' is observed directly after the pH of the storage buffer has been changed. Probably due to the enzyme's hysteretic properties, the 'splitting' increases slightly and reaches a final value (Fig. 2b). In addition to the 'splitting,' a systematic change of the optimum-assay pH values (dashed lines) was observed. It was found that the more basic the

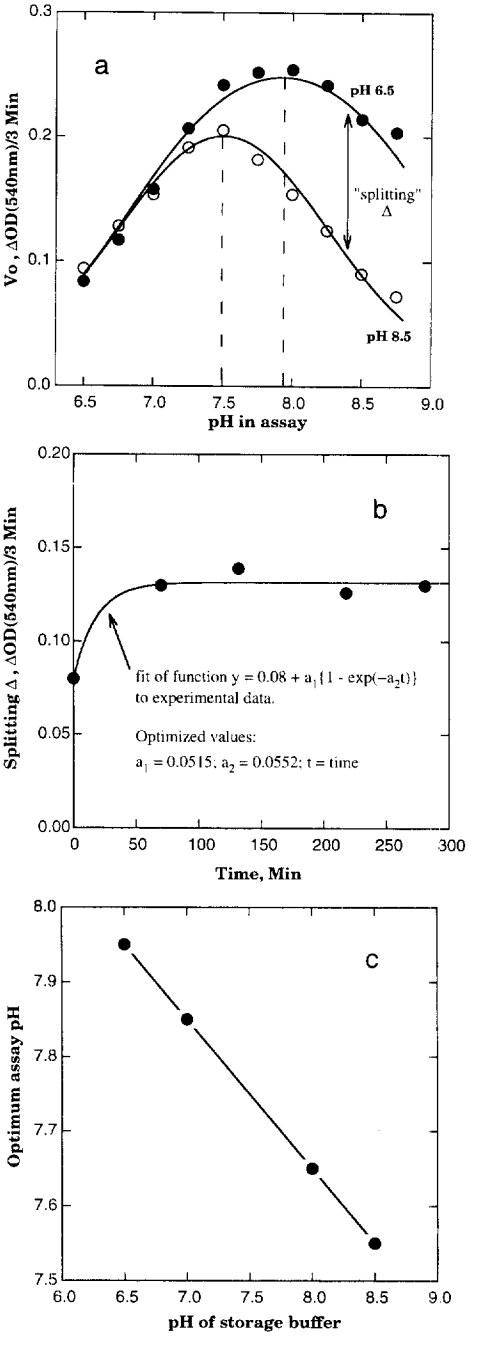

Fig. 2. (a) Solid and open circles show experimental initial velocities (mean of 4 independent experiments) of a NADH (100 μM)–KNO_3 (5 mM)–nitrate reductase system, where divided nitrate reductase samples were stored in 50 mM phosphate buffers (including 3.5 mM cysteine) at pH 6.5 and pH 8.5, respectively. Solid lines show computations from kinetic model. pH 6.5: $K_A^E = K_A^{ES} = 1.4\times10^{-7}$ M; $K_B^E = K_B^{ES} = 1.0\times10^{-9}$ M. pH 8.5: $K_A^E = K_A^{ES} = 1.4\times10^{-7}$ M; $K_B^E = K_B^{ES} = 7.0\times10^{-9}$ M. The assay pH optimum pH_{opt} corresponds to maximum v_0 (dashed lines) and is given by the relationship $pH_{opt} = (1/2)(pK_A^E + pK_B^E)$. (b) 'Splitting' Δ of v_0 at assay pH 8.75 for nitrate reductase stored at pH values 6.5 and 8.5 (see Fig. 2a) as function of storage time. Solid line is a curve fit of experimental data to saturation curve $y = 0.08 + a_1\{1 - \exp(-a_2 \cdot t)\}$. (c) Linear relationship between pH of storage buffer and observed assay pH optimum.

Table 1
Parameter values[a] for different buffer systems

Buffer[b]	K_A^E (M)	K_A^{ES} (M)	K_B^E (M)	K_B^{ES} (M)	K_M (M)	V_{max}^c
K–phosphate	1×10^{-7}	1×10^{-7}	2×10^{-9}	2×10^{-9}	1×10^{-4}	1.1
Tris	2×10^{-7}	1×10^{-6}	2×10^{-8}	3×10^{-9}	1×10^{-4}	0.70
Bis,tris–propane[d]	3×10^{-7}	2×10^{-6}	6×10^{-9}	1×10^{-9}	9×10^{-5}	0.75
Hepes	5×10^{-7}	2×10^{-6}	9×10^{-9}	2×10^{-9}	1×10^{-4}	0.90

[a]See Ref. [26]. Uncertainties of regression parameters: V_{max}, ±10%; K_M, ±5%; $K_{A,B}^{E(S)}$ values, ±30%.
[b]50 mM buffer concentration in assay; enzyme stored in 25 mM tris–HCl buffer, pH 7.5 with 1 mM EDTA and 3.5 mM cysteine.
[c]In $\Delta OD_{540}/3$ min.
[d](1,3-bis[tris(hydroxymethyl]methylamino]propan); $pK_1 = 6.8$; $pK_2 = 9.0$ (25°C).

storage buffer got, the more acidic became the optimum-assay pH (Fig. 2c).

3.2. Presence and absence of cysteine in storage buffer

Cysteine is known to stabilize nitrate reductase preparations and to preserve the high-activity form of the enzyme. According to this, cysteine preserves high (assay) pH optimum values compared with enzyme preparations when no cysteine is present. On the other hand, cysteine is not able to convert a low-activity form (nitrate reductase with a delayed product formation, [14]) to a high-activity form.

In the absence of cysteine, nitrate reductase preparations slowly transform from a high-activity form to a low-activity form with delayed product formation [14]. Nitrate reductase preparations with an increasing extent of hysteresis also show successively decreasing optimum (assay) pH values [18].

3.3. Kinetic parameters from diprotic model

To get information about the nitrate reductase kinetic parameters from the diprotic model, we have measured initial velocities of the purified nitrate reductase. Table 1 shows the various determined parameters. Fig. 3 shows initial velocities v_0 in 50 mM K–phosphate buffer at different initial NO_3^- concentrations and pH values keeping $[NADH]_0$ constant at 100 μM. Solid lines are the result from a nonlinear curve fit of the kinetic parameters to the experimental data points (see legend of Fig. 3 for more details). Besides K–phosphate buffer, we have performed the same kinetic analysis in tris, bis,tris–propane and hepes buffers. The apparent K_M value for nitrate was found to be 100 μM.

It should be noted that in all the studies reported here, nitrate reductase was extracted as a high-active form, i.e., under conditions where the enzyme shows no inhibition with NIP and Mg^{2+}, and is therefore,

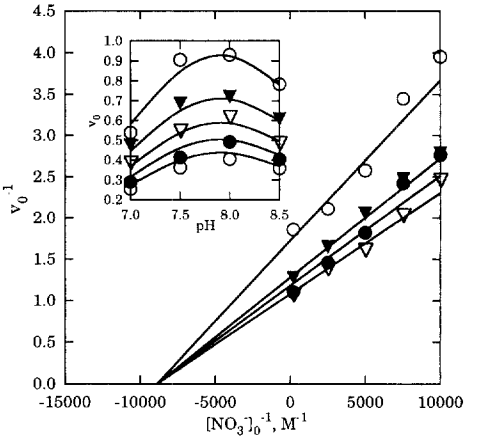

Fig. 3. Inset: Symbols show experimental initial rates v_0 ($\Delta OD_{540}/3$ min) of the nitrate reductase–NADH–nitrate system in phosphate buffer dependent of assay pH when initial nitrate concentration is varied. Nitrate concentrations are (from top to bottom): 5 mM, 400 μM, 200 μM, 135 μM and 100 μM. Initial NADH concentration for all experiments: 100 μM. Solid lines show nonlinear regression fit using the diprotic model. Parameter values are given in Table 1. Main figure: Symbols show experimental double reciprocal values as a function of assay pH. pH values (from top to bottom): 7.0, 8.5, 7.5, 8.0. Straight lines show the calculated double reciprocal lines obtained from optimized parameter values (Table 1) of the diprotic model. Optimization of parameters were done by the commercial plotting programme, SigmaPlot [26]. For the phosphate buffer system the condition $K_A^E = K_A^{ES}$ was used to get the intersection point on the abscissa.

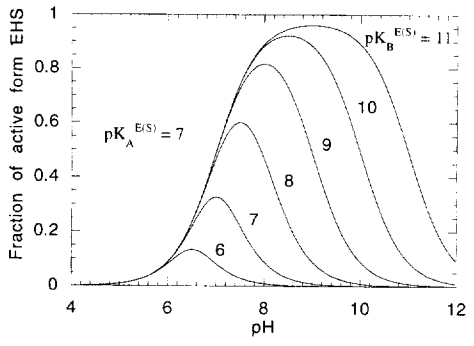

Fig. 4. The fraction of active form f_{EHS} of enzyme EHS^- in diprotic model as a function of pH, $f_{EHS} = [S]/(M_1 K_M + M_2 [S])$. For definition of M_1 and M_2 see Section 2.2.

according to present theories [10,11], not phosphorylated at the regulatory serine (Fig. 1). Consequently, the low-activity form obtained during hysteresis [14] is neither phosphorylated at this site.

Typical to all velocity (v_0)–pH curves is that at low-assay pH values, the curves approach each other, while at higher pH they split (Fig. 2a). The explanation of the 'splitting' can be made with the diprotic model by an increased dissociation of the second proton of species EH^- and EHS^-. In the diprotic model the reaction velocity v can be calculated from the fraction f_{EHS} of the active form of the enzyme, EHS^-, i.e., $v = k_2[E]_0 f_{EHS}$. Fig. 4 shows that a change in $K_B^{E(S)}$ can describe the experimental behavior: increasing $K_B^{E(S)}$ values show a decrease in the optimum-assay pH, while a 'splitting' in f_{ESH} occurs at higher (assay) pH. The physical origin of the 'splitting' may be related to a change in the enzyme's conformation dependent upon storage pH. At high-storage pH, it might be energetically more favorable for the enzyme to have an open conformation (Fig. 1b) and expose more dissociable protons to the medium (which otherwise would be buried in the enzyme's interior). The result would be an increase of solvation energy due to the H^+–OH^- reaction. Probably also more than two protons determine the activity state of the enzyme. In the diprotic model the first proton dissociation may be unaffected by a conformational change, because the dissociation site is already exposed to the medium. The second proton in the diprotic model probably reflects proton dissociation sites that become increasingly exposed to the medium as the enzyme's conformation becomes more open (Fig. 1b). This could at least qualitatively explain the increasing $K_B^{E(S)}$ values with increasing storage pH.

Why is Fig. 2c linear? As indicated above, $K_B^{E(S)}$ may be related to the conformational state or conformational energy of the hydrated enzyme, which again is a function of storage pH. The linearity in Fig. 2c may reflect a linear free energy relationship between $pK_B^{E(S)}$ and $pH_{storage}$. If $pK_A^{E(S)}$ is not dependent upon storage pH (see argument above) then the optimum-assay pH becomes a linear function of storage pH, because $pH_{opt} = (1/2)(pK_A^E + pK_B^E)$. We are not aware of other enzyme systems showing this behavior, but a similar linear relationship between the logarithm of substrate (S) concentration and optimum pH was observed for the *Neurospora crassa* alkaline phosphatase (see Fig. 3 in Ref. [27]). Perhaps also here the linear log $[H^+]_{opt}$ – log [S] relationship reflects a linear free energy relationship between conformational states induced by environmental conditions.

The question, whether the picture of open and closed conformations also applies for the phosphorylated NR–NIP complex will be the subject of further studies.

Acknowledgements

We thank C. MacKintosh and G. Moorhead from the University of Dundee, Scotland, for a sample of NIP. This work was supported by a grant from the Norwegian Research Council NFT.

References

[1] M. Caboche, P. Rouzé, Trends in Genet. 6 (1990) 187.
[2] M. Vincentz, M. Caboche, EMBO J. 10 (1991) 1027.
[3] L.P. Solomonson, M.J. Barber, Annu. Rev. Plant Physiol. Plant Mol. Biol. 41 (1990) 225.
[4] C. Lillo, Plant Sci. 73 (1991) 149.
[5] C. Lillo, Physiol. Plant. 90 (1994) 616.
[6] J.L. Huber, S.C. Huber, W.H. Campbell, M.G. Redinbaugh, Arch. Biochem. Biophys. 296 (1992) 58.
[7] C. MacKintosh, Biochim. Biophys. Acta 1137 (1992) 121.
[8] W.M. Kaiser, S.C. Huber, Plant Physiol. 106 (1994) 817.
[9] W.M. Kaiser, S.C. Huber, Planta 193 (1994) 358.
[10] D. Spill, W.M. Kaiser, Planta 192 (1994) 183.
[11] C. MacKintosh, P. Douglas, C. Lillo, Plant Physiol. 107 (1995) 451.

[12] M. Bachmann, J.L. Huber, P.C. Liao, D.A. Gage, S.C. Huber, FEBS Lett. 387, p. 127.
[13] G. Moorhead, P. Douglas, N. Morrice, M. Scarabel, A. Aitken, C. MacKintosh, Curr. Biol. 6 (1996) 1104.
[14] C. Lillo, P. Ruoff, J. Biol. Chem. 267 (1992) 13456.
[15] C. Frieden, J. Biol. Chem. 245 (1970) 5788.
[16] C. Frieden, Annu. Rev. Biochem. 48 (1979) 471.
[17] K.E. Neet, G.R. Ainslie, Jr., Isotopic probes and complex enzyme systems, in: D.L. Purich (Ed.), Methods of Enzymology, vol. 64, Academic Press, New York, 1980, p. 192.
[18] C. Lillo, Physiol. Plant. 91 (1994) 295.
[19] R.J. Fido, Plant Sci. 55 (1987) 111.
[20] C. Lillo, Physiol. Plant. 57 (1983) 357.
[21] S.G. Waley, Biochim. Biophys. Acta 10 (1953) 27.
[22] K.F. Tipton, H.B.F. Dixon, Initial rate and inhibitor methods, in: D.L. Purich (Ed.), Methods of Enzymology, vol. 63, Academic Press, New York, 1979, p. 183.
[23] I.H. Segel, Enzyme Kinetics. Behavior and Analysis of Rapid Equilibrium and Steady-State Enzyme Systems, Wiley, New York, 1975, p. 884.
[24] C.W. Wharton, R. Eisenthal, Molecular Enzymology, Blackie, Glasgow, 1981, Chap. 6.
[25] A. Cornish–Bowden, Fundamentals of Enzyme Kinetics, Portland Press, London, 1995, p. 187.
[26] SigmaPlot, Scientific Graph System, Version 4.16, Jandel Scientific, Erkrath, Germany, 1991.
[27] F.W. Davis, H. Lees, Can. J. Microbiol. 19 (1973) 135.